Supplemental Material to Stabilizer Tensor Networks: universal quantum simulator on a basis of stabilizer states

Sergi Masot-Llima[1,2] and Artur Garcia-Saez[1,3]

[1] *Barcelona Supercomputing Center, Barcelona 08034, Spain*
[2] *Universitat de Barcelona, Barcelona 08007, Spain*
[3] *Qilimanjaro Quantum Tech, Barcelona 08019, Spain*

(Dated: November 18, 2024)

I. Lemmas and proofs

In this section we state and prove some lemmas from which the *update rules* in the main text are derived. We also include extra comments that do not develop the equations themselves, but are useful when trying to implement the method we present; they will make the reader more familiar with the notation and develop the intuition around the formalism.

A. Representation of a stabilizer state basis

Remember the stabilizer basis $\mathcal{B}(S,D)$ for the sets generated by n stabilizers $\mathcal{S} =< s_1 \dots s_n >$ and n destabilizers $\mathcal{D} =< d_1 \dots d_n >$ corresponds to the states:

$$\mathcal{B}(S,D) = \{\delta_{\hat{i}} |\psi_{\mathcal{S}}\rangle\}_{\hat{i}\in\mathbb{Z}_2^n} = \{d_1^{i_1} \dots d_n^{i_n} |\psi_{\mathcal{S}}\rangle\}_{(i_1,\dots i_n)\in\mathbb{Z}_2^n}. \tag{1}$$

Lemma 1. *For a given stabilizer basis $\mathcal{B}(S,D)$, any state $|\psi\rangle$ in an n-dimensional Hilbert space $\mathcal{H}^n$ can be described as $|\psi\rangle = \sum_i \nu_i \delta_{\hat{i}} |\psi_S\rangle$, where $\hat{i} = (i_1 \dots i_n)$, ν_i are complex coefficients fulfilling $\sum_i |\nu_i|^2 = 1$, and $\delta_{\hat{i}} = d_1^{i_1} \cdot d_2^{i_2} \cdot \dots \cdot d_n^{i_n}$ with respect to the destabilizer generators $d_i \in D$.*

While this property underlies the use of stabilizers in error-correction, and thus can be deduced with their formalism, it can also be seen very concisely entirely within the formalism used in this paper.

Proof: We show that all $\delta_{\hat{i}} |\psi_S\rangle$ are i) normalized and ii) mutually orthogonal, so they form an orthonormal basis, then that iii) the space they generate is the same dimension as the full n-dimensional Hilbert space.

- i) The basis states are normal: $\langle\psi_S| \delta_{\hat{i}}\delta_{\hat{i}} |\psi_S\rangle = \langle\psi_S|\psi_S\rangle = 1$, using that $\delta_{\hat{i}} \in \mathcal{P}^n$ implies $(\delta_{\hat{i}})^2 = Id$.
- ii) The basis states are orthogonal: If we take two different states $\delta_{\hat{i}} |\psi_S\rangle$, $\delta_{\hat{j}} |\psi_S\rangle$, then there is a stabilizer generator $d_k \in D$ such that $i_k = 1, j_k = 0$ or $i_k = 0, j_k = 1$. Taking the first case without loss of generality, the stabilizer generator s_k anticommutes with $\delta_{\hat{i}}$ and commutes with $\delta_{\hat{j}}$, so that

$$\langle\psi_S| \delta_{\hat{i}}\delta_{\hat{j}} |\psi_S\rangle = \langle\psi_S| \delta_{\hat{i}}\delta_{\hat{j}} s_k |\psi_S\rangle = -\langle\psi_S| \delta_{\hat{i}} s_k \delta_{\hat{j}} |\psi_S\rangle = -\langle\psi_S| s_k \delta_{\hat{i}}\delta_{\hat{j}} |\psi_S\rangle = -\langle\psi_S| \delta_{\hat{i}}\delta_{\hat{j}} |\psi_S\rangle \tag{2}$$

  Therefore $\langle\psi_S| \delta_{\hat{i}}\delta_{\hat{j}} |\psi_S\rangle = 0$.

- iii) The basis generates a space of dimension 2^n: since there are n destabilizers d_i, $\hat{i} = (i_1 \dots i_n)$ can take 2^n different values, so the basis $\{\delta_{\hat{i}} |\psi_S\rangle\}_{\hat{i}}$ has that many elements.

□

Other than the basic structure, we need to understand how arbitrary gates modify $|\psi\rangle$ and $|\nu\rangle$. First, we check how different gates are decomposed into the gates of the basis $\mathcal{B}(\mathcal{S},\mathcal{D})$. Then, we find which operations they correspond to within this formalism. We can see from the definition of the stabilizer basis (Eq. 1) that a destabilizer $\delta_{\hat{u}} = d_1^{u_1} \dots d_n^{u_n}$ takes us from one element of the basis to another.

$$\delta_{\hat{u}} |\psi\rangle = \delta_{\hat{u}} \sum_{i=0}^{2^n-1} \nu_i \delta_{\hat{i}} |\psi_{\mathcal{S}}\rangle = \sum_{i=0}^{2^n-1} \nu_i \delta_{\hat{i}+\hat{u}} |\psi_{\mathcal{S}}\rangle = \sum_{i=0}^{2^n-1} \nu_{i+u} \delta_{\hat{i}} |\psi_{\mathcal{S}}\rangle . \tag{3}$$

On the other hand, the multiplication of a stabilizer $\sigma_{\hat{v}} = s_1^{v_1} \dots s_n^{v_n}$ introduces a sign depending on the element of the basis due to anticommutation. Notice that, because d_i only anticommutes with s_i, checking the commutativity of $\delta_{\hat{u}}$ and $\sigma_{\hat{v}}$ is as simple as doing the inner product $\hat{u} \cdot \hat{v}$, which are boolean vectors.

$$\sigma_{\hat{v}} |\psi\rangle = \sum_{i=0}^{2^n-1} \nu_i \sigma_{\hat{v}} \delta_{\hat{i}} |\psi_{\mathcal{S}}\rangle = \sum_{i=0}^{2^n-1} \nu_i (-1)^{\hat{i}\cdot\hat{v}} \delta_{\hat{i}} \sigma_{\hat{v}} |\psi_{\mathcal{S}}\rangle = \sum_{i=0}^{2^n-1} (-1)^{\hat{i}\cdot\hat{v}} \nu_i \delta_{\hat{i}} |\psi_{\mathcal{S}}\rangle . \tag{4}$$

These are equivalent to X and Z operations, respectively, on the computational basis. Therefore, on $|\nu\rangle$ we have:

$$\delta_{\hat{u}} |\psi\rangle = X_{\hat{u}} |\nu\rangle \quad , \quad \sigma_{\hat{v}} |\psi\rangle = Z_{\hat{v}} |\nu\rangle . \tag{5}$$

B. Applying unitaries on the stabilizer TN

Using that $\mathcal{S} \cup \mathcal{D}$ generates $\mathcal{P}^n$, we can decompose any operator as:

$$\mathcal{U} = \sum_i \phi_i \delta_{\hat{u}_i} \sigma_{\hat{v}_i}. \tag{6}$$

The observations in I A tell us how to apply each factor individually, but any decomposition with more than one term is more complicated. Observe that the difference between the update on $|\psi\rangle$ and on $|\nu\rangle$ is only the changing basis, therefore the transformation to $|\nu\rangle$ must also be a unitary operation. This means that our tensor network representation can use the same tools as with circuit simulation, even if the equivalency is not trivial. The following lemma shows us one useful instance.

Lemma 2. *For a given stabilizer basis $\mathcal{B}(S, D)$, any unitary that can be decomposed in the form*

$$\mathcal{U} = \phi_1 \delta_{\hat{u}_1} \sigma_{\hat{v}_1} + \phi_2 \delta_{\hat{u}_2} \sigma_{\hat{v}_2}, \tag{7}$$

is equivalent, in the stabilizer tensor network formalism, to a change of basis with Clifford gates $\delta_{\hat{u}_1}\sigma_{\hat{v}_1}$ followed by a single multi-qubit rotation over the X,Y and Z axes on $|\nu\rangle$:

$$\mathcal{R}_{X_{I_x} Y_{I_y} Z_{I_z}}(2\theta) = \cos(\theta) I - i \sin(\theta) X_{I_x} Y_{I_y} Z_{I_z}, \tag{8}$$

with $\theta = \arccos(Re(\phi_1))$. Using $\circ_h$ [1] , the chosen axes I_x,I_y and I_z related to $\delta_{\hat{u}_1}, \sigma_{\hat{v}_1}, \delta_{\hat{u}_2}, \sigma_{\hat{v}_2}$ as follows:

$$I_y = (\hat{u}_1 + \hat{u}_2) \otimes_h (\hat{v}_1 + \hat{v}_2) \quad , \quad I_x = (\hat{u}_1 + \hat{u}_2) + I_y \quad , \quad I_z = (\hat{v}_1 + \hat{v}_2) + I_y \tag{9}$$

To improve the clarity of the following proof, we abuse the notation and refer to operators $\delta_{\hat{u}_i}$,$\sigma_{\hat{v}_j}$ simply as δ_i, σ_j, and then use the product of operators themselves $\delta_i \cdot \sigma_j$ to mean the product of their defining vectors $\hat{u}_i \cdot \hat{v}_j$; we can do this because there aren't any multiplications of Pauli operators. This helps to keep track of the equations without remembering which operator carries which index. Remember that with this notation, $\delta \cdot \sigma = 1$ when the operators anticommute and 0 when they commute, and also that any (de)stabilizer is hermitian. This notation is used in the rest of the subsection for consistency.

Proof: It can be checked that unitarity implies the following conditions:

$$\begin{aligned} \mathcal{U}^\dagger \mathcal{U} = I &\iff (\phi_1^* \sigma_1^\dagger \delta_1^\dagger + \phi_2^* \sigma_2^\dagger \delta_2^\dagger)(\phi_1 \delta_1 \sigma_1 + \phi_2 \delta_2 \sigma_2) = \phi_1^* \phi_1 I + \phi_2^* \phi_2 I + \phi_2^* \phi_1 \sigma_2 \delta_2 \delta_1 \sigma_1 + \phi_1^* \phi_2 \sigma_1 \delta_1 \delta_2 \sigma_2 = \\ &= (\phi_1^* \phi_1 + \phi_2^* \phi_2) I + (\phi_2^* \phi_1 (-1)^{(\sigma_2 \cdot \delta_2 + \delta_1 \cdot \sigma_2 + \delta_2 \cdot \sigma_1 + \sigma_1 \cdot \delta_1)} + \phi_1^* \phi_2) \sigma_1 \delta_1 \delta_2 \sigma_2 = I \\ &\iff \begin{cases} \phi_1 \phi_1^* + \phi_2 \phi_2^* = 1 \\ \phi_2^* \phi_1 (-1)^{(\delta_1 + \delta_2)\cdot(\sigma_1 + \sigma_2)} = -\phi_1^* \phi_2 \end{cases} . \end{aligned} \tag{10}$$

The first condition tells us that we can rewrite the coefficients with trigonometric functions. We can also factorize the complex phase like $\phi_1 = e^{i\varphi_1} \cos(\theta)$ and $\phi_2 = e^{i\varphi_1} e^{i\omega} \sin(\theta)$, and ignore the term $e^{i\varphi_1}$ as a global phase. Substituting this in the second condition:

$$\begin{aligned} e^{-i\omega} \sin(\theta)\cos(\theta)(-1)^{(\delta_1+\delta_2)\cdot(\sigma_1+\sigma_2)} &= -\cos(\theta) e^{i\omega} \sin(\theta) \rightarrow \\ \rightarrow e^{2i\omega} = (-1)^{(\delta_1+\delta_2)\cdot(\sigma_1+\sigma_2)+1} &\rightarrow e^{i\omega} = \pm(-i)^{(\delta_1+\delta_2)\cdot(\sigma_1+\sigma_2)+1}. \end{aligned} \tag{11}$$

We can also rewrite the unitary as:

$$\mathcal{U} = (\cos(\theta)I + e^{i\omega}\sin(\theta)\delta_2\sigma_2\ \delta_1\sigma_1)\ \delta_1\sigma_1 = (\cos(\theta)I + e^{i\omega}\sin(\theta)(-1)^{\delta_1\cdot\sigma_2}\delta_2\delta_1\ \sigma_2\sigma_1)\ \delta_1\sigma_1. \tag{12}$$

As we have seen in Eqs. 3,4, we treat a (de)stabilizer operator as a set of Z (X) gates. Therefore, the Pauli operator $\delta_1\sigma_1$ to the right is strictly a Clifford update (in fact, with only X,Y and Z gates) that we can apply first. It's left to check that the remaining factor behaves like a rotation.

$$\tilde{\mathcal{U}} = \cos(\theta)I + e^{i\omega}\sin(\theta)(-1)^{\delta_1\cdot\sigma_2}\delta_2\delta_1\ \sigma_2\sigma_1 \tag{13}$$

Similarly, applying $\sigma_{\hat{s}_i}$ ($\delta_{\hat{d}_j}$) is equivalent to the transformation $Z_{\hat{s}_i}$ ($X_{\hat{d}_j}$), and doing two such transformations consecutively is as simple as adding the boolean vectors: $Z_{\hat{s}_j}Z_{\hat{s}_i} = Z_{\hat{s}_j+\hat{s}_i}$. With I_x,I_y and I_z defined as above, one can check that

$$\begin{gathered} I_x + I_y = \hat{\delta}_1 + \hat{\delta}_2 \to X_{I_x+I_y} = \delta_2\delta_1 \\ I_y + I_z = \hat{\sigma}_1 + \hat{\sigma}_2 \to Z_{I_y+I_z} = \sigma_2\sigma_1 \\ I_y = (\hat{\delta}_1 + \hat{\delta}_2) \circ_h (\hat{\sigma}_1 + \hat{\sigma}_2) \to |I_y| = \sum_{a\in I_y} a = (\hat{\delta}_1 + \hat{\delta}_2)\cdot(\hat{\sigma}_1 + \hat{\sigma}_2) \end{gathered}, \tag{14}$$

which is almost the form in Eq.8. Notice that I_x has the unique 1s of $\hat{d}_1 + \hat{d}_2$, with 0s elsewhere, I_z those of $\hat{s}_1 + \hat{s}_2$, whereas I_y has the common 1s between $\hat{d}_1 + \hat{d}_2$ and $\hat{s}_1 + \hat{s}_2$. The use of the Hadamard product (element-wise multiplication) enables the closed form description of I_y. Since $X \cdot Z = -iY$, we can rewrite 8 as

$$\mathcal{R}_{X_{I_x}Y_{I_y}Z_{I_z}}(2\theta) = \cos(\theta)I + \sin(\theta)(-i)^{|I_y|+1}X_{I_x+I_y}Z_{I_y+I_z}. \tag{15}$$

Putting eq.14 and eq.11 together means that the sinus term has the correct phase to be a unitary, so the proposed transformation is indeed a rotation and its coefficients relate to the original unitary as stated. The sign can always be changed with the angle of rotation, so we are done. □

The values v_i of the vectors I_x (I_y,I_z) indicate that we rotate qubit i over X (Y,Z) if $v_i = 1$, and we do nothing if $v_i = 0$. Notice that this gate can be implemented with a cascade of CNOT gates on the affected qubits and a single qubit rotation, plus the appropriate basis changes from X to Y, Z [2]. In particular, we implement the rotation on the innermost affected qubit and add CNOT cascades to each side. And example can be seen in Fig. 2. Lemma 2 is very useful because the basic R_X, R_Y and R_Z gates have this form, so we know how to update with any non-clifford single qubit gate. With the $|\nu\rangle$ notation, lemma 2 can be summarized with:

$$\mathcal{U}|\psi\rangle = (\phi_1\delta_1\sigma_1 + \phi_2\delta_2\sigma_2)|\psi\rangle = \mathcal{R}_{X_{I_x}Y_{I_y}Z_{I_z}}(2\theta)|\nu\rangle \tag{16}$$

In the algorithm, we have to check the value of $\delta_1 \cdot \sigma_2$ to get the sign of the transformation angle right.

We also have a corollary that tells us what the free operations are, which is needed to identify the resource:

Corollary 2.1. *In the context of stabilizer simulation as a resource theory, the free operations depend on the basis $\mathcal{B}(S, D)$ and correspond to $\mathcal{U} = cos(\theta/2)\alpha\delta\sigma + isin(\theta/2)d_is_i\alpha\delta\sigma$, where $d_i \in D$, $s_i \in S$ are generators and $P = \alpha\delta\sigma$ is the decomposition of a Pauli matrix P into $\mathcal{B}(S, D)$.*

Proof: Since it fits the conditions of lemma 2, we apply first the Pauli operator P, which consists only of Clifford gates. Then, since $d_is_i|\psi_S\rangle = d_i|\psi_S\rangle$ is an element of the basis, using 9, we see that $\cos(\theta/2) + i\sin(\theta/2)d_is_i$ is equivalent to a single qubit rotation $R_X(-\theta)$ on $|\nu\rangle$, which does not increase its bond dimension. □

This setup can be extended to decompositions of unitaries into more than two terms. Following [3], a unitary

$$\mathcal{U} = \sum_{i=k}^{L}\phi_k\delta_k\sigma_k, \tag{17}$$

can be implemented with the rotations and coefficients

$$\mathcal{U} = \prod_{k=1}^{L} e^{i\theta_k/2\delta_k\sigma_k}\prod_{k=L}^{1} e^{i\theta_k/2\delta_k\sigma_k}, \qquad \theta_k = \arcsin\frac{\phi_k}{\sqrt{\sum_{j=1}^{k}\phi_j^2}}. \tag{18}$$

Ignoring the initial change of basis of Lemma 2, Eq. 8 is essentially the implementation of rotation

$$\mathcal{U}_{rot} = \phi_1 I + \phi_2 \delta_1\sigma_1\delta_2\sigma_2 = \phi_1 I + \phi_2' \delta_3\sigma_3 = e^{i\theta_{rot}\delta_3\sigma_3}, \tag{19}$$

which means that it can be used to implement each rotation in Eq. 18 individually and, therefore, $\mathcal{U}$.

C. Applying a measurement on the stabilizer TN

For an observable $\mathcal{O} = \alpha\delta_{\hat{n}}\sigma_{\hat{m}}$ we have:

$$\begin{aligned}\langle\psi|\mathcal{O}|\psi\rangle = \langle\psi_{\mathcal{S}}| \sum_{\hat{j}} \nu_{\hat{j}}^*\delta_{\hat{j}}^*\ \alpha\delta_{\hat{n}}\sigma_{\hat{m}} \sum_{\hat{i}} \nu_{\hat{i}}\delta_{\hat{i}}\,|\psi_{\mathcal{S}}\rangle = \sum_{\hat{i},\hat{j}} \alpha\nu_{\hat{j}}^*\nu_{\hat{i}}(-1)^{\hat{m}\cdot\hat{i}}\,\langle\psi_{\mathcal{S}}|\delta_{\hat{j}}\delta_{\hat{n}}\delta_{\hat{i}}|\psi_{\mathcal{S}}\rangle = \\ = \sum_{\hat{i},\hat{j}} \alpha\nu_{\hat{j}}^*\nu_{\hat{i}}(-1)^{\hat{m}\cdot\hat{i}}\Delta_{\hat{j},\hat{i}+\hat{n}} = \alpha\sum_{\hat{i}}(-1)^{\hat{m}\cdot\hat{i}}\nu_{\hat{i}+\hat{n}}^*\nu_{\hat{i}},\end{aligned} \tag{20}$$

where Δ is a Kronecker delta. This is much simpler on $|\nu\rangle$:

$$\langle\psi|\mathcal{O}|\psi\rangle = \alpha\,\langle\nu|X_{\hat{n}}Z_{\hat{m}}|\nu\rangle\,. \tag{21}$$

Notice that the α phase comes from forcing a specific decomposition on $\mathcal{B}(\mathcal{S},\mathcal{D})$, which might mean we have to write $XZ = -iY$ instead of Y directly; it does not mean we allow non-physical observables, that is, with non-real expected values. A measurement of this observable $\mathcal{O}$ projects the state $|\psi\rangle$:

$$|\psi\rangle \to \frac{I \pm \mathcal{O}}{2}\,|\psi\rangle\,. \tag{22}$$

The sign is + (−) when projecting to the positive $|\psi_+\rangle$ (negative $|\psi_-\rangle$) eigenstate. We can calculate $\langle\mathcal{O}\rangle$ with Eq. 21 and randomly decide the output with probability $p = \frac{1+\langle\mathcal{O}\rangle}{2}$ for $|\psi_+\rangle$ and $1-p = \frac{1-\langle\mathcal{O}\rangle}{2}$ for $|\psi_-\rangle$. Then the following lemma shows how to update the coefficients.

Lemma 3. *For a given stabilizer basis $\mathcal{B}(S,D)$ and an observable $\mathcal{O}$ that decomposes as*

$$\mathcal{O} = \alpha\delta_{\hat{n}}\sigma_{\hat{m}}, \tag{23}$$

the projection $\langle I \pm \mathcal{O}\rangle\,2$ onto the positive (negative) eigenstate is equivalent to the following non-unitary operation on $|\nu\rangle$:

$$P_k \cdot \tilde{\mathcal{R}}_{X_{I_x}Y_{I_y}Z_{I_z}} = P_k \cdot \left(\frac{1}{\sqrt{2}}I \pm \frac{\alpha(-i)^{|I_y|}}{\sqrt{2}}X_{I_x}Y_{I_y}Z_{I_z}\right), \tag{24}$$

where k is the position of the first 1 in $\hat{n}$, P_k is the projector $|0\rangle\langle 0|$ on qubit k, and the choice of rotation axes is given by $\delta_{\hat{n}}, \sigma_{\hat{m}}$ as

$$I_y = \hat{n} \circ_h \hat{m} \quad , \quad I_x = \hat{n} + I_y \quad , \quad I_z = \hat{m} + I_y \tag{25}$$

The resulting state $|\psi'\rangle$ is a valid quantum state when renormalized as $\sqrt{\frac{2}{1\pm\langle\psi|\mathcal{O}|\psi\rangle}}\,|\psi'\rangle$.

Proof: We can expand the projection of $\frac{I\pm\mathcal{O}}{2}$ into:

$$\frac{I \pm \mathcal{O}}{2}\,|\psi\rangle = \frac{1}{2}\sum_{\hat{i}}(I \pm \alpha\delta_{\hat{n}}\sigma_{\hat{m}})\nu_{\hat{i}}\delta_{\hat{i}}\,|\psi_{\mathcal{S}}\rangle = \frac{1}{2}\sum_{\hat{i}}(\nu_{\hat{i}} \pm \alpha(-1)^{\hat{i}\cdot\hat{m}}\nu_{\hat{i}+\hat{n}})\delta_{\hat{i}}\,|\psi_{\mathcal{S}}\rangle\,. \tag{26}$$

Then we must consider the update to the stabilizer basis. When $\hat{n} = 0$, we are projecting onto a stabilizer of $|\psi_{\mathcal{S}}\rangle$ and there is no update to $\mathcal{B}(\mathcal{S},\mathcal{D})$. In this case we are directly left with:

$$\frac{I \pm \mathcal{O}}{2}\,|\psi\rangle = \frac{1}{2}\sum_{\hat{i}}\nu_{\hat{i}}(1 \pm \alpha(-1)^{\hat{i}\cdot\hat{m}})\delta_{\hat{i}}\,|\psi_{\mathcal{S}}\rangle \quad \text{if } \hat{n} = 0. \tag{27}$$

In the case $\delta_{\hat{n}} \neq 0$, it was shown in [4] how to update the basis in terms similar to our Eq. 26. Adapting those results to our notation for $|\nu\rangle$, we get the new basis $\mathcal{B}'(\mathcal{S}', \mathcal{D}')$ and :

$$\frac{I \pm \mathcal{O}}{2} |\psi\rangle = \sum_{\hat{i}} \left[\frac{1}{2} (\pm\alpha(-1)^{\hat{i}\cdot\hat{m}})^{\hat{i}_k} \nu_{\hat{i}} \right] \delta'_{\hat{i}+\hat{i}_k\cdot\hat{n}} |\psi_{\mathcal{S}'}\rangle \quad \text{if } \hat{n} \neq 0, \tag{28}$$

where k is the position of the first 1 in $\hat{n}$ and $\hat{i}_k$ the k^{th} element of $\hat{i}$. Notice that $\hat{i}_k = 0$ implies $(\hat{i} + \hat{n})_k = 1$, that is, $\delta_{\hat{i}+\hat{i}_k\cdot\hat{n}} = \delta_{\hat{i}}$ and $\delta_{(\hat{i}+\hat{n})+(\hat{i}+\hat{n})_k\cdot\hat{n}} = \delta_{(\hat{i}+\hat{n})+\hat{n}}$, so the coefficient $\frac{1}{2}(\alpha(-1)^{\hat{i}\cdot\hat{m}})^{\hat{i}_k}\nu_{\hat{i}}$ stays in $\delta_{\hat{i}} |\psi_{\mathcal{S}}\rangle$ and $\frac{1}{2}(\alpha(-1)^{(\hat{i}+\hat{n})\cdot\hat{m}})^{(\hat{i}+\hat{n})_k}\nu_{\hat{i}+\hat{n}}$ moves to $\delta_{(\hat{i}+\hat{n})+\hat{n}} |\psi_{\mathcal{S}}\rangle = \delta_{\hat{i}} |\psi_{\mathcal{S}}\rangle$, leaving $\nu_{\hat{i}+\hat{n}}$ empty; for $\hat{i}_k = 1$ both coefficients concentrate on $\nu_{\hat{i}+\hat{n}}$ and leave $\nu_{\hat{i}}$ empty instead: the measurement halves the non-zero coefficients whenever $\hat{n} \neq 0$. This means we can rewrite the above as:

$$\frac{1 \pm \mathcal{O}}{2} |\psi\rangle = \sum_{\hat{i}} \Delta_{\hat{i}_k,0} \left(\frac{1}{\sqrt{2}} \nu_{\hat{i}} \pm \frac{\alpha(-1)^{\hat{i}\cdot\hat{m}}}{\sqrt{2}} \nu_{\hat{i}+\hat{n}} \right) \delta_{\hat{i}} |\psi_{\mathcal{S}}\rangle \quad \text{if } n \neq 0. \tag{29}$$

where the Kronecker delta filters the non-zero coefficients. Defining $\hat{i}_k \equiv 0$ when $\hat{n} = 0$, we see the only difference between Eq. 27 and Eq. 29 is a factor of $\sqrt{2}$. Since we have to normalize at the end anyway, we can rejoin both cases and proceed with Eq. 29. In terms of $|\nu\rangle$, we can prepare the superposition on all states, which looks almost like a rotation:

$$\tilde{\mathcal{R}} |\nu\rangle = \tilde{\mathcal{R}} \sum_i \nu_{\hat{i}} = \sum_i \frac{1}{\sqrt{2}} \nu_{\hat{i}} \pm \frac{\alpha(-1)^{\hat{i}\cdot\hat{m}}}{\sqrt{2}} \nu_{\hat{i}+\hat{n}}, \tag{30}$$

and remove the duplicate coefficients *afterwards* with a projection on the $|0\rangle$ state of qubit k:

$$P_k = I_0 \otimes \dots I_{k-1} \otimes \begin{pmatrix} 1 & 0 \\ 0 & 0 \end{pmatrix} \otimes I_{k+1} \cdots \otimes I_n \equiv |0\rangle \langle 0|_k , \tag{31}$$

so that $\frac{I+\mathcal{O}}{2} |\nu\rangle = P_k \tilde{\mathcal{R}} |\nu\rangle$. This transformation is similar to the rotation in lemma 2, but removing the i phase. We can reuse the derivation there to find:

$$\tilde{\mathcal{R}}_{X_{I_x} Y_{I_y} Z_{I_z}} = \frac{1}{\sqrt{2}} I \pm \frac{\alpha(-i)^{|I_y|}}{\sqrt{2}} X_{I_x} Y_{I_y} Z_{I_z}, \tag{32}$$

where I_x, I_y, I_z are related to $\delta_{\hat{n}}, \sigma_{\hat{m}}$ exactly as in Eq. 25. Now, I_x has the unique 1s of $\hat{n}$, with 0s elsewhere, I_z those of $\hat{m}$, whereas I_y has the common 1s between $\hat{n}$ and $\hat{n}$. Although it is not a unitary operation, it's equivalent to a projection, so the output is not normalized but is otherwise a valid state. To find the normalization term, we reuse Eq. 20:

$$\langle\psi|\mathcal{O}|\psi\rangle = \alpha \sum_{\hat{i}} (-1)^{\hat{i}\hat{m}} \nu^*_{\hat{i}+\hat{n}} \nu_{\hat{i}} = \alpha^* \sum_{\hat{i}} (-1)^{\hat{i}\hat{m}} \nu^*_{\hat{i}} \nu_{\hat{i}+\hat{n}}. \tag{33}$$

The second equality is a consequence of $\langle\psi|\mathcal{O}|\psi\rangle$ being real. Now:

$$\begin{aligned}
\mathcal{N}^2 &= \left(\langle\psi_{\mathcal{S}}|\,\frac{1\pm\mathcal{O}^\dagger}{2}\right)\left(\frac{1\pm\mathcal{O}}{2}\,|\psi_{\mathcal{S}}\rangle\right) = \\
&= \sum_{\hat{i},\hat{j}} \langle\psi_{\mathcal{S}}|\,\delta_{\hat{j}}\left(\frac{1}{\sqrt{2}}\nu_{\hat{j}}^* \pm \frac{\alpha^*(-1)^{\hat{j}\cdot\hat{m}}}{\sqrt{2}}\nu_{\hat{j}+\hat{n}}^*\right)\Delta_{\hat{j}_k,0}\Delta_{\hat{i}_k,0}\left(\frac{1}{\sqrt{2}}\nu_{\hat{i}} \pm \frac{\alpha^*(-1)^{\hat{i}\cdot\hat{m}}}{\sqrt{2}}\nu_{\hat{i}+\hat{n}}\right)\delta_{\hat{i}}\,|\psi_{\mathcal{S}}\rangle = \\
&= \sum_{\hat{i},\hat{j}} \Delta_{\hat{j}_k,0}\Delta_{\hat{i}_k,0}\left(\frac{1}{\sqrt{2}}\nu_{\hat{j}}^* \pm \frac{\alpha^*(-1)^{\hat{j}\cdot\hat{m}}}{\sqrt{2}}\nu_{\hat{j}+\hat{n}}^*\right)\left(\frac{1}{\sqrt{2}}\nu_{\hat{i}} \pm \frac{\alpha^*(-1)^{\hat{i}\cdot\hat{m}}}{\sqrt{2}}\nu_{\hat{i}+\hat{n}}\right)\langle\psi_{\mathcal{S}}|\delta_{\hat{j}}\delta_{\hat{i}}|\psi_{\mathcal{S}}\rangle = \\
&= \sum_{\hat{i},\hat{j}} \Delta_{\hat{j}_k,0}\Delta_{\hat{i}_k,0}\left(\frac{1}{2}\nu_{\hat{j}}^*\nu_{\hat{i}} \pm \frac{\alpha^*(-1)^{\hat{j}\cdot\hat{m}}}{2}\nu_{\hat{j}+\hat{n}}^*\nu_{\hat{i}} \pm \frac{\alpha(-1)^{\hat{i}\cdot\hat{m}}}{2}\nu_{\hat{j}}^*\nu_{\hat{i}+\hat{n}} + \frac{|\alpha|^2}{2}v_{\hat{j}+\hat{n}}^*v_{\hat{i}+\hat{n}}\right)\Delta_{\hat{i},\hat{j}} = \\
&= \sum_{\hat{i}} \Delta_{\hat{i}_k,0}\left(\frac{1}{2}|\nu_{\hat{i}}|^2 + \frac{|\alpha|^2}{2}v_{\hat{i}+\hat{n}}^*v_{\hat{i}+\hat{n}} \pm \frac{\alpha^*(-1)^{\hat{i}\cdot\hat{m}}}{2}\nu_{\hat{i}+\hat{n}}^*\nu_{\hat{i}} \pm \frac{\alpha(-1)^{\hat{i}\cdot\hat{m}}}{2}\nu_{\hat{i}}^*\nu_{\hat{i}+\hat{n}}\right) = \\
&= \frac{1}{2}\sum_{\hat{i}} \Delta_{\hat{i}_k,0}|\nu_{\hat{i}}|^2 + \frac{1}{2}\sum_{\hat{i}} \Delta_{\hat{i}_k,0}|\nu_{\hat{i}+\hat{n}}|^2 \pm \sum_{\hat{i}} \Delta_{\hat{i}_k,0}\,\langle\psi|\mathcal{O}|\psi\rangle = \\
&= \frac{1}{2}\sum_{\hat{i}} (\Delta_{\hat{i}_k,0} + \Delta_{(\hat{i}+\hat{n})_k,0})|\nu_i|^2 \pm \frac{1}{2}\,\langle\psi|\mathcal{O}|\psi\rangle = \frac{1\pm\langle\psi|\mathcal{O}|\psi\rangle}{2}.
\end{aligned} \tag{34}$$

We used that $\hat{i}_k = 0 \leftrightarrow (\hat{i}+\hat{n})_k = 1$ again, so the sum of $(\Delta_{\hat{i}_k,0} + \Delta_{(\hat{i}+\hat{n})_k,0})$ is always 1. Because $(\hat{i}+\hat{n})+\hat{n} = \hat{i}$, each contribution to the sum appears twice, so the Kronecker delta selects one of each pair and is thus equivalent to the factor $\frac{1}{2}$ in front of the expected value. This equation proves we have a valid quantum state in all cases with a renormalization term of:

$$\mathcal{N} = \sqrt{\frac{1\pm\langle\psi|\mathcal{O}|\psi\rangle}{2}}. \tag{35}$$

□

We can implement the rotation we found with a CNOT cascade similarly to Eq. 8, but instead of a central R_X rotation we need the following one-qubit (non-unitary) operation:

$$\tilde{\mathcal{R}} = \frac{1}{\sqrt{2}}\begin{pmatrix} 1 & \pm\alpha(-i)^{|I_y|} \\ \pm\alpha(-i)^{|I_y|} & 1 \end{pmatrix}. \tag{36}$$

II. Examples of Pauli decompositions

The notion of which gates are entangling is related to how we decompose a given Pauli matrix in the stabilizer basis. To understand our proposal better, we showcase this decomposition on a few examples of well-known stabilizer states. The trivial case happens for the computational basis, since the stabilizer set are the single qubit Z_i operators and the destabilizer set the X_i operators. We compare this to the 1D cluster state and the 2D Toric code, which have some notion of locality in their basis but still allow us to see the effect of different dimensions, and finally we create a few non-local examples to work on extreme cases. These are summarized in Table II. Notice that the numbering starts of destabilizers starts on 0 to be consistent with the basis states.

The 1D cluster state [5], which has applications for Measurement-based Quantum computing [6] for n qubits can be prepared with the following gates

$$\mathcal{U}_C\,|\psi_0\rangle = \left(\prod_{j=1}^{n-1} C_j Z_{j+1}\right)\left(\mathcal{H}^{\otimes n}\right)|0\ldots0\rangle\,. \tag{37}$$

Since U_C is a Clifford circuit, it also sets the destabilizer generators d_i which define the basis $\mathcal{B}(\mathcal{S},\mathcal{D})$. This means we can use U_C to trace any δ_i to a corresponding δ_i^0 in the basis $\mathcal{B}'$ of the starting state $|\psi_0\rangle$. Thus, the elements of the basis are:

$$\delta_{\hat{i}}\,|\psi_S\rangle = U_C\delta_{\hat{i}}^0U_C^\dagger U_C\,|\psi_0\rangle = U_C X_{\hat{i}}\,|0\ldots0\rangle = U_C\,|i\rangle\,. \tag{38}$$

We can thus know the stabilizers and destabilizers using U_C on those of the computational basis above, $s_i = Z_i$ and $d_i = X_i$. Because the Hadamard layer switches the role of X and Z, and a CZ gate turns XI (IX) into XZ (ZX), it is easy to check that $s_i = Z_{i-1}X_iZ_{i+1}$ and $d_i = Z_i$ If the chain is not periodic, the only exception is $s_0 = X_0Z_1$ and $s_n = Z_{n-1}X_n$. This implies non-local Paulis become slightly more non-local, adding operators at each side of the "original" Pauli operators, as seen in Table II. The operator with X operators in all qubits becomes $(-1)^n d_1 s_1 s_2 \cdots s_{n-1} s_n d_n$, so it also stays n-local.

The Toric code [7], which is useful for quantum error correcting codes [8], consists of a periodic grid where edges represent qubits, vertices represent operators $X_aX_bX_cX_d$ on the 4 edges it connects, and tiles represent operators $Z_aZ_bZ_cZ_d$ on its 4 adjacent edges. The error correcting involves working with states that are stabilized by this operators. Thus, we can define a stabilizer space with them, although this setup does not describe a single state because its purpose is to encode logical qubits in its degrees of freedom. By adding 2 arbitrary stabilizers to the list (see Table II) we can fix the stabilizer space to a single state to have a working stabilizer basis $\mathcal{B}(\mathcal{D}, \mathcal{S})$. The resulting stabilizer state $|\psi_{\mathcal{S}}\rangle$ can be prepared from the $|0\rangle$ computational state with projections onto the stabilizer space using the stabilizers with X operators (which we order to be the last $n/2$):

$$\prod_{j=n/2}^{n-1} (I + s_j) \, |0\rangle^{\otimes n} = \mathcal{M}_{TC}^n \, |0\rangle^{\otimes n} \, . \tag{39}$$

For our example, we pick a small size of 2×2 tiles to deal with readable Pauli operators, and number the edges from left to right and top to bottom. The decomposition of operators in this setup shows a great variance in locality. Some local operators like X_1 stay local (d_1), but others like X_4 become very non-local ($d_0d_2s_4s_6s_7$). For 2-local operators we see a similar behaviour, with some increasing a lot their locality (X_4X_6 becomes $d_0d_3s_5s_6s_7$) and others diminishing it (Z_5Z_6 becomes d_8). For which operators this happens is highly dependent on the size and ordering of qubits chosen. However, in all cases we find non-local operators with Pauli weight 4, which is the amount of non-identity Pauli operators that it contains, that become local; they correspond to the stabilizers that define the Toric code. As an example, the tile with stabilizer $Z_0Z_4Z_6Z_7$ decomposes as s_3.

As a very non-local example, we can make a stabilizer basis for which all local operators in one basis become maximally non-local (n-local). We show both the odd case and the even case, which are slightly different in the stabilizers but have similar behaviour. First, any local operator X_i,Z_i is n-local. For larger operators, the locality depends on the parity of their Pauli weight. Operators of even weight maintain it in the stabilizer decomposition (for example, X_3X_7 decomposes to d_3d_7), and also maintain locality in our example. The order of the stabilizers in our example could be rearranged to change this notion of locality, however; we comment on this kind of changes after the examples, below. Operators with odd weight, instead, become weight n and n-local in all cases.

The difference between the odd and even cases is that the stabilizer generator set has to be arranged slightly differently to ensure commutativity rules between them. A consequence is that one of the basis in the even case is not n-local – Y in our example. We show that this is a limitation of the even case and cannot be improved, and not caused by our choice of $\mathcal{S}, \mathcal{D}$. For $X_i = \prod_{k=1}^n x_k^i$ and $Z_i = \prod_{k=1}^n z_k^i$ to both be n-local, then for all k, $x_k^i, z_k^i \in \{s_k, d_k, d_k s_k\}$, that is, all sites have a destabilizer or stabilizer and are not "empty". Since they must anticommute, for some k $x_k^i = z_k^i$, otherwise they would differ at all sites and $X_iZ_i = (-1)^n Z_iX_i = Z_iX_i$. Therefore $y_k^i = z_k^i x_k^i = 1$ and is "empty" at site k, so not n-local.

One could try to improve locality by changing the labels of each stabilizer (such that, for instance, an operator decomposing into s_3s_7 decomposes into s_3s_4). This is equivalent to the ordering of qubits in the encoding scheme of any quantum algorithm, which can be very impactful in fermionic mappings [9] among other problems. Similarly, two different generator sets, even if they define the same $\mathcal{S}$ (and therefore the same state $|\psi_{\mathcal{S}}\rangle$), lead to different generators of $\mathcal{D}$. These define the "order" of the elements in the basis, meaning which quantum state $|\psi\rangle$ is labeled by which element $|i\rangle$ in the basis of the stabTN. For example, in the *symmetric non-local* case, the stabilizer state is $|\psi_{\mathcal{S}}\rangle = |0\cdots0\rangle$, but the first destabilizer is $d_0 = IX\cdots X$, unlike the computational basis. This means the stabTN with coefficients $|\nu\rangle = 1/\sqrt{2}(|0\cdots00\rangle + |0\cdots01\rangle) = 1/\sqrt{2}(I + d_0)\,|0\cdots00\rangle$, which is separable, is encoding the entangled state $1/\sqrt{2}(|0\cdots00\rangle + |1\cdots10\rangle)$. Of course, trying to simplify a convoluted stabilizer basis such as this one mid-computation would change $|\nu\rangle$ in non-trivial ways.

Basis (n qubits)	s_i	d_i	X_i	Z_i	X_iX_{i+1}		$X_1X_2...X_{n-1}X_n$
Computational $\{\|i\rangle\}_{i=0}^{2^n-1}$	Z_i	X_i	d_i	s_i	d_id_{i+1}		$d_1d_2\cdots d_{n-1}d_n$
Cluster state $\{\mathcal{U}_C\|i\rangle\}_{i=0}^{2^n-1}$	$Z_{i-1}X_iZ_{i+1}$	Z_i	$d_{i-1}s_id_{i+1}$	d_i	$d_{i-1}s_id_id_{i+1}s_{i+1}d_{i+2}$		$d_1s_1s_2\cdots s_{n-1}s_nd_n$
Maximally non-local (n odd) $\{\delta_{\hat{i}}\|0\rangle^{\otimes n}\}_{i=0}^{2^n-1}$	$XZZ\cdots ZZ$ $ZXZ\cdots ZZ$ $\cdots$ $ZZZ\cdots ZX$	$ZYY\cdots YY$ $YZY\cdots YY$ $\cdots$ $YYY\cdots YZ$	$s_1d_1...s_i\hat{d_i}...s_nd_n$	$s_1...\hat{s_i}...s_n$	X_iX_{i+1} d_id_{i+1}	$X_{i-1}X_iX_{i+1}$ $s_1\cdots s_nd_1\cdots \hat{d}_{i-1}\hat{d}_i\hat{d}_{i+1}\cdots d_n$	$s_1s_2\cdots s_{n-1}s_n$
Maximally non-local (n even) $\{\delta_{\hat{i}}\|0\rangle^{\otimes n}\}_{i=0}^{2^n-1}$	$YXX\cdots XX$ $XYX\cdots XX$ $\cdots$ $XXX\cdots XY$	$YZZ\cdots ZZ$ $ZYZ\cdots ZZ$ $\cdots$ $ZZZ\cdots ZY$	$s_1\cdots s_nd_i$	$s_id_1...d_n$	d_id_{i+1}	$s_1\cdots s_n$ $d_{i-1}d_id_{i+1}$	$d_1d_2\cdots d_{n-1}d_n$
Toric code $(2\times 2, n=8)$ $\{\delta_{\hat{i}}\mathcal{M}_{TC}^8\|0\rangle^{\otimes 8}\}_{i=0}^{255}$	$ZIZZZIII$ $IZZZIZII$ $ZIIIZIZZ$ $IIZIIIZI$ $XXXIIIXI$ $XXIXIIIX$ $IIXIXXXI$ $IXIIIXII$	$XIIIIIIX$ $IXIIIIII$ $IIIIIIIX$ $IIXXIIII$ $IIIIZIZI$ $IIZZIIZI$ $IIIIZIII$ $IIIIZZII$	X_1: d_1 X_4: $d_0d_2s_4s_6s_7$	d_6d_7	X_4X_6: $d_0d_3s_5s_6s_7$	Z_5Z_6: d_8 $Z_0Z_4Z_6Z_7$: s_3	s_6s_7

TABLE I. Summary of decomposition examples for operators with different localities in a selection of stabilizer bases. These bases are either extreme cases (*computational basis* as trivial and *Maximally non-local* as complex) or stabilizer states that are relevant in the field (cluster state, 2×2 Toric code). From left to right, we show the name of the example and its basis, the stabilizer generators, the destabilizer generators, up to 3 1-local operators, up to 3 slightly non-local operators, and 1 n-local example. For the toric code we give explicit examples, whereas for the rest we find and show the general case. We use a hat $\hat{}$ on any (de)stabilizer $\hat{d}$ to indicate that it's missing when multiplying a series of (de)stabilizers from 1 to n. Also, the phases of the decomposition are omitted for simplicity.

III. Entangling power of an arbitrary gate

There is not a unique way to define the entangling power of a gate. There are many notions of multipartite entanglement that one can use, and the entanglement of the final state depends on the initial state. This means one usually looks at an average over all possible states [10] or a worst/best case, which can also complicate the calculation of the chosen metric. Since we use an MPS, we focus on the bipartite entanglement case, and instead of the average, we find the maximum bond dimension χ' needed in our MPS after applying a gate on an MPS that had maximum bond dimension χ. We use the Schmidt decomposition of unitaries [11], which has been used previously to characterize arbitrary gates [12] and tells us we can decompose any unitary as

$$\mathcal{U} = \sum_{i=1}^{k} s_i A_i \otimes B_i, \tag{40}$$

where $s_i \geq 0$, $\sum_i |s_i|^2 = 1$ and A_i, B_i are an orthogonal operator basis [13]. When applying the rotation $\mathcal{R}$ in Eq. 8, we can focus on any arbitrary bond of our MPS by decomposing it as in Fig. 1. This way, we only need to check how the gates that cross the chosen bond affect χ.

With the Schmidt decomposition [14] of the initial state $|\psi\rangle$ as:

$$|\psi\rangle = \sum_{i=1}^{\chi} \lambda_i |\psi_A^i\rangle \otimes |\psi_B^i\rangle, \tag{41}$$

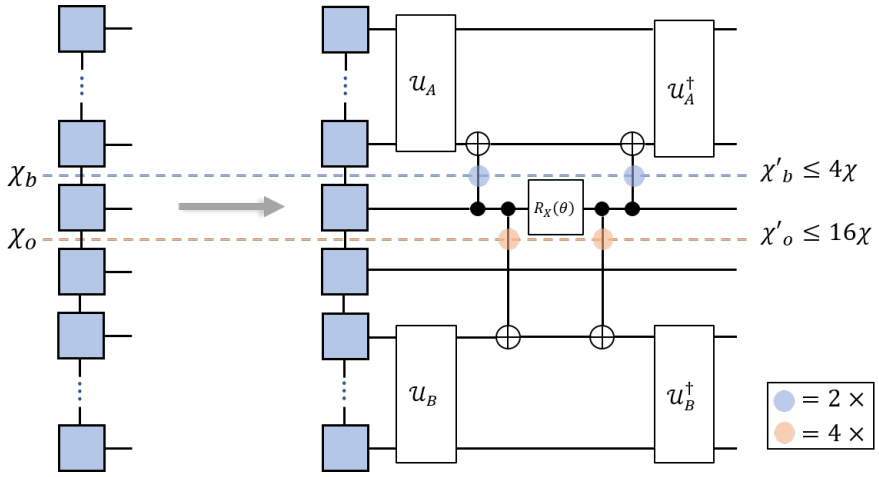

FIG. 1. Possible decomposition of the rotation 8 showcasing how the gates affect χ for different bonds. All gates that can be grouped into a unitary on partition A (B) are irrelevant. The bond in blue starts with χ_b and each CNOT can increase it by at most a factor of 2, reaching $\chi'_b \leq 4\chi_b$ after the transformation. For the orange bond, starting with χ_o, the implementation of a CNOT across far away qubits on an MPS requires that we apply a SWAP gate at each line crossing, which increases χ by at most 4, so that at the end we have $\chi'_o \leq 16\chi_o$. This argument is independent of the initial bonds.

limited to rank χ, applying a two qubit gate with Schmidt number k means we get that χ' is at most:

$$\mathcal{U}_k |\psi\rangle = \sum_{j=1}^{k} \sum_{i=1}^{\chi} (s_j \lambda_i) A_j |\psi_A^i\rangle \otimes B_j |\psi_B^i\rangle \,. = \sum_{i=1}^{k\chi} \tilde{\lambda}_i |\phi_A^i\rangle \otimes |\phi_B^i\rangle \tag{42}$$

The final form is still a valid Schmidt decomposition thanks to the orthonormality of A_i, B_i and $\sum_i s_k^2 = 1$. A CNOT gate has Schmidt number $k = 2$ [13], so the set of two CNOTs that are applied to a particular bond can increase at most $\chi' \leq 4\chi$. Counter to intuition, the worst-case scenario when using an MPS is not an update that affects all qubits, but one that affects qubits that are far apart: a CNOT gate over tensors that are not neighbours is implemented with SWAPs on our MPS. A SWAP gate has Schmidt rank 4, so Eq. 42 gives the bound $\chi' \leq 16\chi$ instead, as stated in the main text. Since this maximum is a consequence of SWAP gates, TN geometries other than MPS that adapt to the connectivity of the simulated circuit can reduce the bound to 4χ; this entails a bigger complexity in the TN contraction, as is the case in general for higher dimensional networks.

IV. Stabilizer TN update example

It is useful to illustrate an example of a coefficient update with a non-Clifford gate in terms of $|\nu\rangle$. We take an arbitrary basis $\mathcal{B}(\mathcal{S}, \mathcal{D})$ for 5 qubits and a unitary that decomposes as

$$\mathcal{U} = \frac{\sqrt{3}}{2}\delta_{\hat{d}_1}\sigma_{\hat{s}_1} + \frac{1}{2}\delta_{\hat{d}_2}\sigma_{\hat{s}_2} = \left(\cos(\pi/6) + \sin(\pi/6)\delta_{\hat{d}_2}\sigma_{\hat{s}_2}\delta_{\hat{d}_1}\sigma_{\hat{s}_1}\right)\delta_{\hat{d}_1}\sigma_{\hat{s}_1} = \left(\cos(\pi/6) - \sin(\pi/6)(\delta_{\hat{d}_2}\delta_{\hat{d}_1})(\sigma_{\hat{s}_2}\sigma_{\hat{s}_1})\right)\delta_{\hat{d}_1}\sigma_{\hat{s}_1}. \tag{43}$$

Let us assume that the vector representation of δ, σ is:

$$\left.\begin{array}{l}\hat{d}_1 = (1,1,0,0,0)\\ \hat{d}_2 = (1,0,0,1,0)\end{array}\right\} \rightarrow \hat{d}_2\hat{d}_1 = (0,1,0,1,0)$$
$$\left.\begin{array}{l}\hat{s}_1 = (0,0,0,1,0)\\ \hat{s}_2 = (0,0,1,0,0)\end{array}\right\} \rightarrow \hat{s}_2\hat{s}_1 = (0,0,1,1,0) \tag{44}$$

which also implies $\hat{d}_1 \cdot \hat{s}_2 = 1$. Then using Eqs. 3,4 and the $|\nu\rangle$ notation we can rewrite

$$\mathcal{U} |\nu\rangle = (\cos(\pi/6) - \sin(\pi/6)(X_1X_3)(Z_2Z_3))\, X_0X_1Z_3 |\nu\rangle = (\cos(\pi/6) + i\sin(\pi/6)X_1Y_3Z_2)\, X_0X_1Z_3 |\nu\rangle \tag{45}$$

We see that this fits Eq. 8. Then the coefficients can be updated with the corresponding multiqubit rotation, which we show in Fig. 2. We also show the decomposition that we have used in our Python implementation, which uses two cascades centred on the middle qubit instead of a single CNOT cascade.

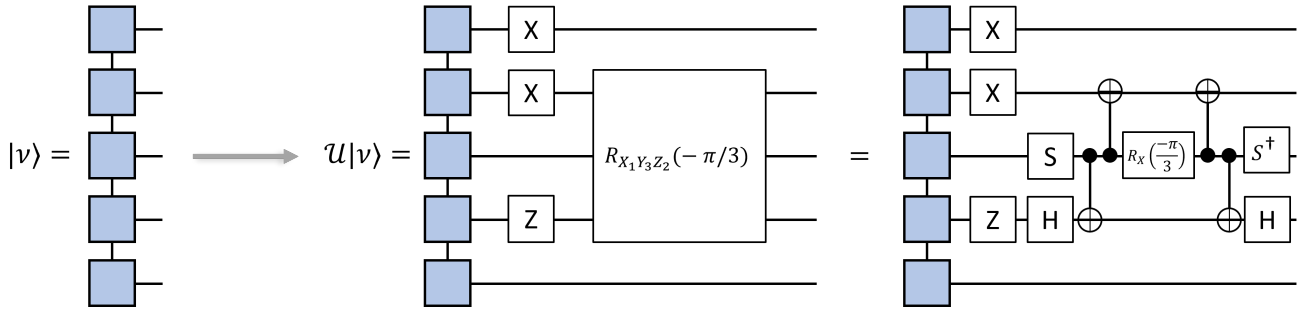

FIG. 2. Example of coefficient update for the unitary described in Eq. 43. Horizontal lines are "qubit" sites in the traditional MPS tensor network representation of a quantum state. Gates are applied from left to right. The resulting TN of this example is more entangled than the initial $|\nu\rangle$.

Most circuit simulations compile an input gate set into a specific set of gates, since practical realizations of quantum computers are similarly bound by a limited set of native gates. Our simulation approach can handle any circuit with a $\{CNOT, R_X, R_Y, R_Z\}$ decomposition, so it's compatible with most circuits despite the limitations of lemma 2. Other characterizations are possible and still compatible with the stabilizer TN framework, but the implementation of unitaries of arbitrary decomposition is left for future work.

---

[1] Hadamard multiplication is an element wise multiplication of two tensors a and b of the same shape, such that the entries of the result c follow: $c_{i_1\ldots i_n} = (a \circ_h b)_{i_1\ldots i_n} = a_{i_1\ldots i_n} \cdot b_{i_1\ldots i_n}$.

[2] M. B. Mansky, V. R. Puigvert, S. L. Castillo, and C. Linnhoff-Popien, Decomposition Algorithm of an Arbitrary Pauli Exponential through a Quantum Circuit (2023), 2305.04807.

[3] A. F. Izmaylov, T.-C. Yen, R. A. Lang, and V. Verteletskyi, Unitary partitioning approach to the measurement problem in the variational quantum eigensolver method (2019), arXiv:1907.09040 [quant-ph].

[4] T. J. Yoder, A generalization of the stabilizer formalism for simulating arbitrary quantum circuits (2012).

[5] H. J. Briegel and R. Raussendorf, Persistent entanglement in arrays of interacting particles, Phys. Rev. Lett. **86**, 910 (2001).

[6] R. Raussendorf and H. J. Briegel, A one-way quantum computer, Phys. Rev. Lett. **86**, 5188 (2001).

[7] A. Kitaev, Fault-tolerant quantum computation by anyons, Annals of Physics **303**, 2 (2003).

[8] R. Acharya, L. Aghababaie-Beni, I. Aleiner, T. I. Andersen, M. Ansmann, F. Arute, K. Arya, A. Asfaw, N. Astrakhantsev, J. Atalaya, R. Babbush, D. Bacon, B. Ballard, J. C. Bardin, J. Bausch, A. Bengtsson, A. Bilmes, S. Blackwell, S. Boixo, G. Bortoli, A. Bourassa, J. Bovaird, L. Brill, M. Broughton, D. A. Browne, B. Buchea, B. B. Buckley, D. A. Buell, T. Burger, B. Burkett, N. Bushnell, A. Cabrera, J. Campero, H.-S. Chang, Y. Chen, Z. Chen, B. Chiaro, D. Chik, C. Chou, J. Claes, A. Y. Cleland, J. Cogan, R. Collins, P. Conner, W. Courtney, A. L. Crook, B. Curtin, S. Das, A. Davies, L. D. Lorenzo, D. M. Debroy, S. Demura, M. Devoret, A. D. Paolo, P. Donohoe, I. Drozdov, A. Dunsworth, C. Earle, T. Edlich, A. Eickbusch, A. M. Elbag, M. Elzouka, C. Erickson, L. Faoro, E. Farhi, V. S. Ferreira, L. F. Burgos, E. Forati, A. G. Fowler, B. Foxen, S. Ganjam, G. Garcia, R. Gasca, Élie Genois, W. Giang, C. Gidney, D. Gilboa, R. Gosula, A. G. Dau, D. Graumann, A. Greene, J. A. Gross, S. Habegger, J. Hall, M. C. Hamilton, M. Hansen, M. P. Harrigan, S. D. Harrington, F. J. H. Heras, S. Heslin, P. Heu, O. Higgott, G. Hill, J. Hilton, G. Holland, S. Hong, H.-Y. Huang, A. Huff, W. J. Huggins, L. B. Ioffe, S. V. Isakov, J. Iveland, E. Jeffrey, Z. Jiang, C. Jones, S. Jordan, C. Joshi, P. Juhas, D. Kafri, H. Kang, A. H. Karamlou, K. Kechedzhi, J. Kelly, T. Khaire, T. Khattar, M. Khezri, S. Kim, P. V. Klimov, A. R. Klots, B. Kobrin, P. Kohli, A. N. Korotkov, F. Kostritsa, R. Kothari, B. Kozlovskii, J. M. Kreikebaum, V. D. Kurilovich, N. Lacroix, D. Landhuis, T. Lange-Dei, B. W. Langley, P. Laptev, K.-M. Lau, L. L. Guevel, J. Ledford, K. Lee, Y. D. Lensky, S. Leon, B. J. Lester, W. Y. Li, Y. Li, A. T. Lill, W. Liu, W. P. Livingston, A. Locharla, E. Lucero, D. Lundahl, A. Lunt, S. Madhuk, F. D. Malone, A. Maloney, S. Mandrá, L. S. Martin, S. Martin, O. Martin, C. Maxfield, J. R. McClean, M. McEwen, S. Meeks, A. Megrant, X. Mi, K. C. Miao, A. Mieszala, R. Molavi, S. Molina, S. Montazeri, A. Morvan, R. Movassagh, W. Mruczkiewicz, O. Naaman, M. Neeley, C. Neill, A. Nersisyan, H. Neven, M. Newman, J. H. Ng, A. Nguyen, M. Nguyen, C.-H. Ni, T. E. O'Brien, W. D. Oliver, A. Opremcak, K. Ottosson, A. Petukhov, A. Pizzuto, J. Platt, R. Potter, O. Pritchard, L. P. Pryadko, C. Quintana, G. Ramachandran, M. J. Reagor, D. M. Rhodes, G. Roberts, E. Rosenberg, E. Rosenfeld, P. Roushan, N. C. Rubin, N. Saei, D. Sank, K. Sankaragomathi, K. J. Satzinger,

H. F. Schurkus, C. Schuster, A. W. Senior, M. J. Shearn, A. Shorter, N. Shutty, V. Shvarts, S. Singh, V. Sivak, J. Skruzny, S. Small, V. Smelyanskiy, W. C. Smith, R. D. Somma, S. Springer, G. Sterling, D. Strain, J. Suchard, A. Szasz, A. Sztein, D. Thor, A. Torres, M. M. Torunbalci, A. Vaishnav, J. Vargas, S. Vdovichev, G. Vidal, B. Villalonga, C. V. Heidweiller, S. Waltman, S. X. Wang, B. Ware, K. Weber, T. White, K. Wong, B. W. K. Woo, C. Xing, Z. J. Yao, P. Yeh, B. Ying, J. Yoo, N. Yosri, G. Young, A. Zalcman, Y. Zhang, N. Zhu, and N. Zobrist, Quantum error correction below the surface code threshold (2024), arXiv:2408.13687 [quant-ph].

[9] T. Parella-Dilmé, K. Kottmann, L. Zambrano, L. Mortimer, J. S. Kottmann, and A. Acín, Reducing entanglement with physically inspired fermion-to-qubit mappings, PRX Quantum **5**, 030333 (2024).

[10] P. Zanardi, C. Zalka, and L. Faoro, Entangling power of quantum evolutions, Physical Review A **62**, 030301(R) (2000).

[11] M. A. Nielsen, C. M. Dawson, J. L. Dodd, A. Gilchrist, D. Mortimer, T. J. Osborne, M. J. Bremner, A. W. Harrow, and A. Hines, Quantum dynamics as a physical resource, Physical Review A **67**, 052301 (2003), quant-ph/0208077.

[12] B. Jonnadula, P. Mandayam, K. Zyczkowski, and A. Lakshminarayan, Entanglement measures of bipartite quantum gates and their thermalization under arbitrary interaction strength, Physical Review Research **2**, 043126 (2020).

[13] S. Balakrishnan and R. Sankaranarayanan, Operator-Schmidt decomposition and the geometrical edges of two-qubit gates, Quantum Information Processing **10**, 449 (2011).

[14] M. A. Nielsen and I. L. Chuang, Introduction to quantum mechanics, in *Quantum Computation and Quantum Information: 10th Anniversary Edition* (Cambridge University Press, 2010) pp. 60–119.